

SHORT THESIS FOR THE DEGREE OF DOCTOR OF PHILOSOPHY (PHD)

Studying substrate binding by P-glycoprotein at different steps of the catalytic cycle and its inhibition by the UIC2 monoclonal antibody

by Gábor Szalóki

Supervisor: Katalin Goda, PhD



UNIVERSITY OF DEBRECEN

DOCTORAL SCHOOL OF MOLECULAR CELL AND IMMUNE BIOLOGY

DEBRECEN, 2018

Studying substrate binding by P-glycoprotein at different steps of the catalytic cycle and its inhibition by the UIC2 monoclonal antibody

by Gábor Szalóki, master of science in molecular biology

Supervisor: Katalin Goda, PhD

Doctoral School of Molecular Cell and Immune Biology, University of Debrecen

Head of the Examination Committee:

Prof. Zsuzsanna Szondy, MD, PhD, DSc

Members of the Examination Committee:

Prof. János Matkó, PhD, DSc

Norbert Szentandrassy, MD, PhD

The examination took place at Discussion Room, Institute of Biochemistry and Molecular Biology, Faculty of Medicine, University of Debrecen at 13 pm 6th October 2015.

Head of the Defense Committee:

Prof. László Fésüs, MD, PhD, DSc, Member of Hung. Acad. of Sci.

Reviewers:

Prof. Balázs Sarkadi, MD, PhD, DSc, Member of Hung. Acad. of Sci.

István Krizbai, MD, PhD, DSc

Members of the Defense Committee:

Prof. János Matkó, PhD, DSc

Prof. Péter Antal-Szalmás, MD, PhD, DSc

The PhD Defense takes place at the Lecture Hall of the Department of Obstetrics and Gynecology, Faculty of Medicine, University of Debrecen at 11 am 8th October 2018.

1 Introduction

The development of resistance against anticancer drugs during chemotherapy is still a severe problem in the every-day oncology practice. Some tumor types are sensitive to the chemotherapeutic drugs in the beginning of treatment, but later on they become more and more resistant to the applied therapy, while other cancers are intrinsically resistant to numerous anticancer drugs they have never met before. Unfortunately, tumors can develop resistance against the majority of anticancer drugs that have different chemical nature and mechanism of action. This phenomenon was called multidrug resistance (MDR) and the causes and possible ways of its prevention or inhibition are intensively studied since the 1970's.

By the second half of the 1980's it was proved, that the MDR phenotype of cancer cells is often related to the presence or increased expression of an active plasma membrane transporter called P-glycoprotein (Pgp). Based on the sequence of its cDNA, Pgp showed significant homology with certain bacterial transporters belonging to the ABC family of transport ATPases, and it became the first human member of the ABC protein superfamily.

Afterwards 48 ABC protein genes were identified in the human genome and they were categorized into seven subfamilies (from ABCA to ABCG). The majority of them is active membrane transporters and thus, often called ABC transporters, while some of them are ion channels or ion channel regulators. However, the members of the ABCE and ABCF subfamilies are not transmembrane proteins. Similarly to Pgp many ABC transporters were proved to be involved in the development of the MDR phenotype, but the first described Pgp remained the "prototype" of multidrug transporters. Therefore, Pgp is subject of a great scientific interest and its function and ways of inhibition are intensively studied.

1.1 The structure and catalytic cycle of Pgp

Pgp is the first member of the B subfamily of human ABC proteins encoded by the *abcb1* (*mdr1*) gene that is located on chromosome 7. It is expressed in tissues of barrier functions (e.g. intestinal epithelium, capillary endothelial cells of the blood-brain barrier, hepatocytes), where it is presumably involved in the protection of our body against xenobiotics. Pgp is a 170 kDa glycoprotein composed of 1280 amino acids. It is a so-called "full transporter", since one continuous polypeptide chain contains its two transmembrane domains (TMDs, each consisting six transmembrane α -helices) and two nucleotide binding domains (NBDs). The TMDs form the substrate binding site which is able to bind and export hundreds of compounds from the cell using the energy provided by ATP binding and hydrolysis carried out by the NBDs. The structure of the NBDs and the mechanism of ATP binding and hydrolysis is unique among ATP utilizing enzymes and transport ATPases. Although, the RecA-like structure of the NBDs containing the Walker A and Walker B sequences can be found in every ATPases, the ABC "signature" motifs are characteristic for the ABC proteins. Another

interesting feature of ABC proteins is the strong cooperation of the two NBDs upon ATP binding and hydrolysis.

Despite accumulating significant amount of functional and structural data about human Pgp, there are no high resolution structures available that are based on x-ray crystallography data. Therefore, in molecule dynamic simulations homology models based on the crystal structures of bacterial ABC transporters or Pgps from mice or *C. elegans* are used. According to these studies two stable conformers of Pgp can be assumed: in the absence of nucleotides, the NBD dimers are dissociated and the TMDs adopt an inward-facing conformation, which make the substrate binding site accessible from the intracellular space or from the inner leaflet of the membrane; while after ATP binding the two NBDs dimerize forming the outward-facing conformation which is closed towards the intracellular side of the membrane and open to the extracellular side. It is supposed that Pgp fluctuates between these two conformations.

According to the general concept explaining the substrate transport by active transporters the substrate binding sites switch from high to low substrate affinity conformation to ensure transport against the concentration gradient. However, it is still unknown whether this affinity change is triggered by ATP hydrolysis or ATP binding itself. Also there is no consensus regarding the number of hydrolyzed ATPs per one catalytic cycle.

To explore the catalytic cycle of Pgp, numerous biochemical experiments were carried out using mutant Pgp variants, in which certain key amino acids of the conserved sequences of one or both NBDs were exchanged. According to literature data, these mutations, depending on which conserved sequence is affected, stabilize the Pgp molecules at different stages of the catalytic cycle and abolish their ATPase activity regardless the mutation affected one or both NBDs. These experiments supported the idea, that the ATP hydrolysis activity of both NBDs is indispensable for Pgp function. This may imply that both catalytic sites should hydrolyze the bound ATP upon the catalytic cycle or alternatively only one ATP is hydrolyzed, but the two nucleotide binding sites should hydrolyze ATP in a strictly alternating manner. On the other hand the NBDs of Pgp molecules crystallized in the absence of substrate and ATP appears to be separated. If this conformation is indeed relevant and part of the catalytic cycle, it is possible that both ATPs are hydrolyzed during the cycle or alternatively after the hydrolysis of the first ATP the second one is unable to keep the NBD dimer together. Due to these contradictory results there is no consensus regarding the details of the catalytic cycle of Pgp in the scientific community.

1.2 Clinical significance of Pgp

Pgp is generally expressed in tissues having barrier functions and it is suggested to have an important role in the protection of the body from toxic substances. In the same time its expression in cancer cell causes multidrug resistance, hereby worsens the prognosis of many types of cancers and decreases the survival of patients. Early studies showed that loss of the *abcb1a/b* genes in mice (homologues of the human *abcb1* gene)

is not accompanied by major physiological consequences. Thus, inhibition of Pgp molecules may be a plausible strategy for overcoming drug resistance without serious side effects. The classical pharmacological approach involves co-administration of cytotoxic compounds that are substrates of Pgp with pump inhibitors to increase the accumulation of the former one into the tumor cells. Unfortunately, upon clinical trials Pgp inhibitors induced unpredictable and intolerable pharmacokinetic interactions probably by inhibiting Pgp molecules expressed in barrier tissues leading to altered pharmacokinetics and increasing toxicity of the co-administered chemotherapeutic agents.

In tumor patients many different resistance mechanisms can contribute to the development of the drug resistant phenotype; therefore their proper identification is crucial from the aspect of choosing the most suitable personalized therapy. On the other hand, it is important to expand the repertoire of therapeutic protocols that are able to overcome multidrug resistance. This also requires the establishment of appropriate models systems that can be used to test the new resistance reversal strategies *in vivo*.

Several monoclonal antibodies (mAb) recognizing extracellular epitopes of Pgp have been developed. A few of them (e.g., MRK16, MRK17, MC57, HYB-241, and UIC2) are thought to recognize discontinuous conformation sensitive epitopes. Upon binding, these antibodies can partially inhibit Pgp mediated drug transport *in vitro* and *in vivo*. However, this inhibitory effect is often weak, its extent may depend on the transported substrate, and it is variable even in the case of the same substrate according to general experience.

UIC2 is a monoclonal antibody that recognizes a complex conformation sensitive epitope on the extracellular part of Pgp. In the absence of Pgp substrates and modulators, UIC2 can bind only to 10–40% of cell surface Pgps, while the rest of Pgp molecules adopts the UIC2 binding conformation only in the presence of a distinct group of substrates or modulators (e.g., cyclosporine A (CsA), SDZ PSC 833, vinblastine and paclitaxel). In previous studies our workgroup has demonstrated that the UIC2 antibody itself completely inhibits Pgp function when it is applied together with any of the above Pgp modulators added at low, sub-inhibitory concentration that makes all cell surface Pgps UIC2 reactive. On the other hand, we also demonstrated in case of human tumors xenotransplanted into severe combined immunodeficient (SCID) mice that UIC2 could readily penetrate into the compact solid tumors, intensively staining cell surface Pgps and increasing daunorubicin accumulation in the Pgp⁺ tumors to the level of the Pgp⁻ ones.

These data rise the question whether the combined application of a class of modulators (including CsA) used at sub-inhibitory concentrations and of the UIC2 antibody can increase the anti-tumor effect of cytostatic drugs (e.g. doxorubicin, daunorubicin) in Pgp expressing tumors and whether clinically relevant decrease in tumor mass can be achieved by the treatment.

2 Objectives

Although the catalytic cycle of Pgp has been intensively studied for more than three decades, the connection between the different steps of the ATPase cycle and the rearrangement of the TMDs, which mediate the transport of the substrates against their concentration gradient, is still unclear. Considering the sensitivity of the ABC transporters to the composition of their membrane environment, opposed to previous studies applying heterologous expression systems or purified proteins, we decided to engineer mammalian cell lines expressing wild-type and mutant human Pgp variants at extremely high level and study them in their natural plasma membrane environment. Using this system we aimed to answer the following questions:

- How does the substrate affinity of the Pgp change during the catalytic cycle?
- How does the replacement of the conserved lysine amino acids of Walker A sequences in one or both NBDs to methionine (K433M and/or K1076M) affect the transport activity of the protein?
- How do the above single and double Walker A mutations affect the transition of the protein between the high and low substrate affinity conformations?

In previous studies our workgroup has demonstrated that binding of the UIC2 antibody completely inhibits Pgp function when it is applied together with certain Pgp modulators, such as cyclosporine A (CsA) added at low, sub-inhibitory concentrations. In the present study we decided to generate and test an *in vivo* model system based on the xenotransplantation of Pgp⁺ and Pgp⁻ tumors into SCID mice. Using this model system we aimed to answer the following questions:

- Whether the combined treatment with CsA and UIC2 mAb can potentiate the anti-tumor effect of doxorubicin (DOX) in Pgp⁺ tumors to achieve clinically relevant reduction in tumor size?
- Whether the partially functional immune system of the SCID mice can contribute to the observed antitumor effect of the combined treatment?

3 Materials and methods

3.1 Ethics statement

In animal experiments the Principles of Laboratory Animal Care (National Institute of Health) was strictly followed, and the experimental protocol was approved by the Laboratory Animal Care and Use Committee of the University of Debrecen (Permission Numbers: 26/2006/DE-MAB and 122/2009/DE-MAB).

The human blood preparations (buffy coats) were obtained from the Debrecen Regional Center of Hungarian National Blood Transfusion Service and the blood plasma samples were donated by healthy volunteers. Written informed consent was obtained from donors prior to blood plasma donation, and their data were processed and stored according to the principles expressed in the Declaration of Helsinki. The experiments were done with the approval of the Scientific and Research Ethics Committee of the Medical Research Council (ETT TUKEB, permission number: 25364-1/2012/EKU (449/P1/12.)).

3.2 Cell lines

In our experiments we used the NIH 3T3 mouse fibroblast cell line and its human *mdr1* gene transfected variant (NIH 3T3 MDR1); KB-3-1 human epidermoid carcinoma cell line and its Pgp⁺ subclone, KB-V-1; MDCK II (Madin-Darby canine kidney) cell line and its ABCG2 expressing variant; GLC4 human small cell lung carcinoma cell line and its MRP1 expressing variant. The mutant Pgp variant (K433M, K1076M and K433M/K1076M) expressing transgenic cell lines were made by our collaboration partners using Sleeping Beauty transposon based expression system and 3T3 and MDCK cell lines.

The cells were grown as adherent cultures at 37 °C in 5% CO₂ atmosphere, in Dulbecco's modified Eagle's medium (DMEM) supplemented with heat-inactivated fetal calf serum, L-glutamine and penicillin-streptomycin cocktail. The high expression of wild type Pgp was maintained by drug selection. Two days before the experiment, the cells were transferred into drug-free medium. Prior use, the cells were removed from the flask bottom by Trypsin-EDTA treatment.

3.3 Direct immunofluorescence staining of Pgp

To label cell surface Pgp molecules, the cell suspension was incubated for 30 minutes at 37 °C with 15D3-A647 or with the combination of UIC2-A647 and cyclosporine A (CsA). Then the cells were washed three times with PBS containing glucose and FCS. The cells were analyzed by FACS Array or FACS Aria III flow cytometers.

3.4 Indirect immunofluorescence staining of cell surface ABC transporters

The cell suspension was incubated for 30 minutes at 37 °C with the appropriate primary antibody. Before labelling with QCLR-3 anti-MRP1 antibody, the cells were fixed and permeabilized, then incubated with the mAb for 30 minutes at 4 °C. Then the samples were washed three times and incubated for 30 minutes on ice with goat anti-

mouse IgG, conjugated with CFL647. Following three washings, the cells were analyzed with FACS Aria III flow cytometer.

3.5 Western blot analysis

Proteins of the whole cell lysate (2.5 µg/sample) were subjected to SDS-polyacrylamide gel electrophoresis on 8% polyacrylamide gel and electro-blotted to 0.45 µm pore size nitrocellulose membrane. Pgp expression was detected by the G1 anti-Pgp mAb and a goat anti-mouse HRP-conjugated IgG secondary antibody, both applied at 1:5,000 dilution. The ECL reaction was carried out with Super Signal West Femto ECL reagent and recorded using a Fluor Chem Q Alpha Innotech gel documentation system.

3.6 Calcein and BODIPY-vinblastine accumulation tests

The cells were pretreated with CsA, and then incubated with calcein acetoxymethyl ester or BODIPY FL-vinblastine (VBL-BPY) for 30 minutes. Following washes, the cells were kept on ice until the analysis. The dead cells were excluded from the analysis by propidium iodide (PI) staining. The transport activity of the Pgp was expressed as relative calcein accumulation increase, which is the fluorescence ratio of the CsA-treated and untreated samples, both corrected with the background fluorescences.

3.7 Rhodamine 123 efflux assay

The cells were incubated with rhodamine 123 (R123, fluorescent Pgp substrate) for 30 minutes. The samples containing wild type Pgp expressing cells also contained verapamil (competitive Pgp inhibitor). The excess R123 was removed by washing and the samples were kept on ice until the analysis. At the beginning of the measurement the cells were diluted with 37 °C R123 free medium and the fluorescence intensity of the cells were recorded continuously of 5 minutes using the temperature controlled sampling unit of the FACS Aria III flow cytometer. Later, after 10, 20, 30, 60 and 120 minutes, the fluorescence of samples were also determined. The data were plotted on a time-fluorescence intensity graph, and the first order rate constant of the R123 efflux was determined by fitting an exponential curve on the data points.

3.8 Labelling of intact cells with VBL-BPY and 15D3-A647

The cells were cultured in 8 chamber Ibidi µ-Slide for two days, using an initial cell number to make a near confluent culture to the time of the experiment. Following three washes, the cells were pretreated with CsA or with the mixture of NaN₃ and 2-deoxy-D-glucose or Na₂VO₃ or N-ethylmaleimide (NEM) for 30 minutes at 37 °C. Then the samples were co-incubated with VBL-BPY and anti-Pgp mAb 15D3, conjugated with A647. At the end of the incubation the cells were washed three times, and then labelled with PI and images were taken using a confocal microscope. The PI positive, dead cells were excluded from the analysis.

3.9 Permeabilization of cells with Staphylococcus aureus α -toxin or streptolysin-O

3T3 and MCDK cells were prepared in Ibidi μ -Slide IV^{0.4} slides for confocal microscopy, were permeabilized by Staphylococcus aureus α -toxin or streptolysin-O (SLO) respectively, with 30-60 minute incubation in the presence of DTT, protease inhibitor cocktail and FCS in HEPES buffer. The ratio of the permeabilized cells was determined by PI staining and we finished the permeabilization when at least the 80% of the cells become PI positive. Then the unbound toxins were removed by washing.

3.10 Labelling of permeabilized cells with VBL-BPY and 15D3-A647

After permeabilization the cells were washed three times, then preincubated for 30 minutes with CsA or the mixture of ATP/MgCl₂ and Na₂VO₃, or AMP-PNP/MgCl₂ followed by staining with VBL-BPY and 15D3-A647 for another 30 minutes. At the end of the incubation, the cells were washed three times, stained with PI and analyzed with confocal microscope. We used the permeabilized, PI positive cells for the analysis.

3.11 *In vitro* cytotoxicity tests

The KB-V1 and BK-3-1 cells were cultured in 96 well plates in drug-free medium for 24 hours, and then different concentrations of doxorubicin (DOX) were added to the appropriate wells together with CsA and/or UIC2 and incubated for further 72 hours. After it the medium was replaced with a fresh AlamarBlue containing one, and two hours later the reduced AlamarBlue content was determined by a microplate reader. The fluorescence intensities of the samples were proportional to the amount of the living cells in them. The ratios of the living cells were plotted against the concentration of the DOX, and after fitting of the dose-response curves, the half effective doses (EC₅₀) of DOX were determined.

3.12 *In vitro* antibody-dependent cell-mediated cytotoxicity (ADCC) assay

Human peripheral blood mononuclear cells (PBMCs) were prepared from the blood of healthy donors by density gradient centrifugation. The PBMC rich fraction (effector cells) was washed two times and re-suspended in DMEM. KB-V1 and KB-3-1 (target cells) cells were labelled with 5(6)-carboxyfluorescein diacetate N-succinimidyl ester (CFDA-SE) for 10 minutes, then washed three times and re-suspended in DMEM.

The target cells were mixed with effector cells at target/effector cell ratios of 1:5, 1:10, 1:50 and 1:100, and then they were incubated in the presence or absence of CsA and/or UIC2 at 37 °C in CO₂ incubator for 8 hours. After labelling with PI, the samples were analyzed by flow cytometer. The CFDA-SE⁺/PI⁺ subpopulation was considered as dead target cells, while CFDA-SE⁺/PI⁻ ones were considered as living cells. The ratios of the CFDA-SE⁺/PI⁺ double positive cells to all CFDA-SE⁺ cells gave the ratio of the dead target cells, which were plotted against the target/effector cell ratios.

3.13 *In vitro* complement-dependent cytotoxicity (CDC) assay

Samples containing KB-V1 or KB-3-1 cells and UIC2 mAb in the presence or absence of CsA were treated with freshly prepared human serum at different dilutions.

The samples were incubated for 4 hours in CO₂ incubator at 37°C then stained with PI and were analyzed by flow cytometer. The hemolytic activity of the applied human sera was determined using sheep red blood cells sensitized with rabbit stroma antibody.

3.14 Animal experiments

10 to 12 week-old, pathogen-free B-17 severe combined immunodeficiency (SCID) mice were used in this study. Animals were housed under pathogen free circumstances, the sterilized food and drinking water were available ad-libitum to all animals.

SCID mice were injected subcutaneously with KB-3-1 and KB-V1 cells. To obtain approximately similar tumor sizes in case of KB-V1 and KB-3-1 cells we had to inject double number of KB-V1 cells, because of their slower cell proliferation rate. Tumors were grown for 4 days and then the mice were treated with DOX alone, or DOX combined with either UIC2 mAb or CsA or both. The animals were killed 8 days after treatment with chemotherapy by cervical dislocation and the tumors were removed to weigh them and then they were snap frozen in liquid nitrogen and stored till mRNA expression analysis.

3.15 mRNA analysis

The frozen tumor sections were equilibrated in 10 volumes pre-chilled RNAlater-ICE solution at -20°C overnight to protect RNA from degradation and then total RNA was isolated. RNA was then subjected to reverse transcription-real time quantitative polymerase chain reaction (RT-qPCR) using the Taqman assay. Pgp mRNA expression was normalized to the human glyceraldehyde-3-phosphate dehydrogenase (GAPDH) expression.

3.16 Confocal laser scanning microscopy

Microscopy samples were analyzed by an Olympus FluoView 1000 confocal microscope equipped with an inverted IX-81 stand and an UPlanSApo 60× (NA=1,35) oil immersion objective. The 488-nm blue line of an argon-ion laser, and the 543-nm green and the 633-nm red helium-neon laser lines were used for the excitation of VBL-BPY, PI and Alexa 647, respectively. Fluorescence intensities were detected in the spectral ranges of 500–530 nm, 555–655 nm and 655–755 nm, respectively.

To assess the co-localization of VBL-BPY (green) and Alexa 647-conjugated 15D3 (red) fluorescence signals, single optical slices of apical membrane surfaces were recorded for double-labelled cells, then the pattern and extent of co-localization in the sections were determined. The Pearson's co-localization index (CI) provides a reliable estimate on the extent of fluorescence co-localization: CI values close to zero indicate no or a very low degree, while the CI = 1 value would correspond to a full overlap between the two colors in each pixel of the image, whereas -1 value means that the presence of a signal from one channel exclude the presence of the signal from the other.

In case of permeabilized cells, due to the changes in the membrane structure we cannot acquire suitable images for CI calculation, therefore fluorescence intensity ratio

of VBL-BPY and 15D3-Alexa-647 was determined in pixels representing the plasma membrane selected on the basis of 15D3-Alexa-647 fluorescence intensity.

3.17 Flow cytometry

We used Becton Dickinson FACScan, FACS Array or FACS Aria III flow cytometers to measure whole cell fluorescence.

In ADCC and CDC experiments a FACScan flow cytometer was used. Its 488 nm, blue laser was used to excite CFDA-SE and PI and the fluorescence intensities were detected through a 530/30 nm and 585/42 nm band-pass filters for CFDA-SE and PI, respectively.

When FACS Array was used, PI was excited by the 532 nm diode laser, while A647 was excited by the 633 nm laser, and the fluorescence intensities were detected through a 585/42 nm and 661/16 nm band-pass filters, respectively.

Calcein, VBL-BPY accumulation and R123 efflux measurements were carried out on a Becton Dickinson FACSAria III Cell Sorter. Calcein, VBL-BPY and R123 were excited by the 488 nm line of a solid state laser and the emitted light was detected using a 502 nm dichroic mirror and a 530/30 nm band-pass filter. PI was excited by a 562 nm laser and the emitted light was detected applying a 590 nm dichroic mirror and a 595/50 nm band-pass filter. Cell populations with high Pgp expression were sorted by FACS Aria III after direct immunofluorescence labelling with 15D3-A647. In this case the A647 dye was excited by a 633 nm laser and the fluorescence was detected through a 660/20 nm band-pass filter.

3.18 Data and statistical analysis

For image analysis ImageJ, Adobe Photoshop and Adobe Illustrator programs were used. Statistical analysis was carried out using SigmaStat or SPSS. Comparison of two groups was carried out by unpaired t-test, statistical significance in the case of three or more groups was assessed using analysis of variance (ANOVA), applying the Holm-Sidak multiple comparison test for post hoc pair-wise comparison of the data. In the case of unequal variances Dunnett T3 post hoc pair-wise comparison method was used. Differences were considered significant at $P < 0.05$.

4 Results

I. Examination of substrate binding of P-glycoprotein during the catalytic cycle

4.1 MDCK cells can express wild type Pgp and its mutant variants at comparable level

To compare the transport activity of the wild type and Walker A mutant Pgps, we needed cell lines that express the protein variants on similar levels. Therefore, we sorted the cell populations with homogenously high Pgp expression using immunofluorescence labelling followed by fluorescence activated cell sorting from the transgenic cell lines made by our collaboration partners. We checked the Pgp expression of the cell clones regularly by Western blot and flow cytometry. The expression level of the wild type and single mutant Pgp expressing cell lines did not differ significantly, while the double mutant Pgp expressing cells showed higher expression.

4.2 Single Walker A mutant Pgps have residual transport activity

We measured the transport activity of the Pgp variants by substrate accumulation tests, using calcein-AM. The transport activity of the Pgp variants was characterized by the CsA (cyclosporine A is a competitive Pgp inhibitor) sensitive calcein uptake.

In the case of the wild type Pgp expressing cells the calcein accumulation of the CsA treated cells was 84.3 ± 7.3 times higher compared to the untreated ones, which reflects the strong transport activity of the wild type Pgp. The relative calcein accumulation increase was much smaller in the case of the single mutant Pgps (12 ± 0.8 fold and 9.5 ± 1.7 fold for the K433M and K1076M mutants, respectively), but still significantly higher than in the double mutant Pgp expressing cells (2.3 ± 0.2 times) or the Pgp non-expressing cells (1.4 ± 0.3 times). Based on it we can assume that the single mutant Pgps have residual transport activity, while the mutation of both NBDs abolishes its transport function.

To provide a quantitative measure of the residual transport activity of the single Walker A mutants, we determined the first order rate constants of rhodamine123 (R123) efflux from the cells. We loaded the cells with R123 and then transferred them into a larger volume of R123 free medium and measured the decrease of the R123 fluorescence in the cells using flow cytometry.

Our results showed that the rate constants in the case of the Pgp non expressing cells ($0.02 \pm 0.01 \text{ min}^{-1}$) and double Walker A mutant Pgp expressing cells ($0.02 \pm 0.01 \text{ min}^{-1}$) were identical and very low. In contrast with it, the values of the single Walker A mutant Pgp expressing cell lines were four times higher ($0.1 \pm 0.02 \text{ min}^{-1}$ and $0.09 \pm 0.01 \text{ min}^{-1}$ in the case of K433M and K1076M cells, respectively), while the wild type Pgp expressing cells exhibited 30 times higher rate constant ($0.7 \pm 0.06 \text{ min}^{-1}$) compared to the Pgp non expressing cells. Taken together these data support the transport activity of single mutants, while the double mutant is inactive.

4.3 The single Walker A mutant Pgps are capable of conformational changes that alter reactivity with UIC2 mAb

According to previous data of our workgroup, UIC2 mAb, when used alone, is able to bind to the 20-40% of the cell surface Pgps, but in the presence of CsA or as the result of ATP depletion all of them become UIC2 reactive. On the other hand, the presence of orthovanadate ion (V_i) reduces the fraction of the UIC2 recognizable Pgps. In our experiments we investigated whether the Walker A mutant Pgp variants are capable of the UIC2 detectable conformation changes. Single mutant Pgp expressing cells, similarly to the wild type expressing ones, showed increased UIC2 reactivity after CsA treatment or ATP depletion, while V_i , which stabilizes the post-hydrolysis transition state by replacing the phosphate ion in the NBD, caused significant decrease in UIC2 reactivity. In contrast with it, double mutant Pgps showed high UIC2 mAb binding regardless of the treatments. Based on these results, we can conclude that the single mutant Pgps are capable of the switch between the UIC2 reactive and non-reactive conformations, while the double Walker A mutant Pgps are stabilized in the UIC2 reactive conformation, and did not respond to the applied treatments.

4.4 Modulators do not alter the amount of the cell surface Pgps

Since most of the modulators used in our experiments may have a significant effect on the metabolism of cells, we checked whether they affect the cell surface expression of Pgps. Therefore, we pretreated the cells with the Pgp modulators and then labelled them with 15D3 mAb, which recognizes a conformation insensitive extracellular epitope of Pgp. Based on these experiments we concluded that the used modulators did not alter the cell surface Pgp expression level in the course of the labelling experiments.

4.5 Single Walker A mutant Pgps are capable of switching between high and low substrate affinity conformations

We demonstrated in substrate accumulation tests, that the BODIPY-FL conjugated variant of vinblastine (VBL-BPY), similarly to vinblastine, retained its Pgp substrate character. Investigating the cellular distribution of VBL-BPY we have found that it accumulated in intracellular vesicles in the Pgp⁻ MDCK cells and no membrane staining could be observed. Consistently with the effective Pgp-mediated efflux of vinblastine-bodipy (VBL-BPY), the cells expressing WT Pgp showed significantly lower levels of intracellular fluorescence as compared to the Pgp⁻ cells. ATP-depleted cells overexpressing wild-type Pgp showed increased intracellular fluorescence and more interestingly sequestered VBL-BPY in the plasma membrane as well. Strikingly, weak plasma membrane sequestration of VBL-BPY was also observed in cells transfected with single Walker A mutant Pgp variants, while double Walker A mutant Pgp expressing cells showed strong membrane staining. Addition of CsA, a competitive inhibitor of Pgp, prevented plasma membrane accumulation of VBL-BPY, suggesting that the enrichment of VBL-BPY in the plasma membrane is in each case due to its high-affinity binding to Pgp.

Since the signal of the VBL-BPY and the 15D3 mAb used to visualize Pgps correlated well, the fraction of the Pgps in substrate binding conformation could be determined by calculating the Pearson's cross-correlation coefficients of the two signals. The antibody staining was unchanged in the course of the treatments supporting that the cross-correlation coefficients depend mostly on VBL-BPY binding to Pgp. In cells expressing double Walker A mutant Pgp large cross-correlation coefficients close to unity (~ 0.8) indicate that the majority of Pgp molecules are in high substrate affinity conformation. Competitive inhibitor (CsA) was able to prevent plasma membrane sequestration of VBL-BPY in all Pgp expressing cell lines, resulting in low cross correlation coefficients. Single Walker A mutants also exhibited somewhat increased drug binding compared to the WT, but this binding was fully suppressed by transition state analogs, e.g. vanadate. Furthermore, ATP depletion by Na-azide or prevention of ATP binding by NEM treatment shifted both single mutant and WT Pgp variants into the substrate binding conformation, as reflected by increased co-localization of VBL-BPY and Pgp molecules in the plasma membrane. Remarkably, the high substrate affinity of double mutant Pgp was not affected by any of the above treatments.

These results suggest that the single Walker A mutant Pgp variants are capable of switching between the high and low substrate affinity conformations, while the double mutant is stabilized in the high substrate affinity state.

4.6 Nucleotide binding is sufficient to switch Pgp from high to low drug affinity conformation

Since nucleotides are not membrane permeable, their effect on the conformation and substrate affinity of Pgp molecules cannot be studied in intact cells. Therefore, we permeabilized the NIH 3T3 MDR1 cells with Staphylococcus α -toxin and the MDCK cell lines with Streptolysin-O, washed out the nucleotides, and then we co-incubated the cells with nucleotides and modulators followed by staining with VBL-BPY and 15D3-A648 anti-Pgp mAb. Then the ratio of the VBL-BPY and 15D3-A648 fluorescence was calculated in pixels representing the plasma membrane. Similarly to the previous experiments, the binding of 15D3-A647 was constant, the ratio of the fluorescence signals depended exclusively on the binding of VBL-BPY.

In permeabilized cells ATP depletion synchronized WT Pgp molecules in a high drug binding affinity conformation, as indicated by VBL-BPY sequestration in the plasma membrane. This tight binding of VBL-BPY to Pgp was reversed in the presence of ATP and vanadate, consistent with the low drug binding affinity of the transition state complex. Strikingly, incubation of permeabilized cells with 5 mM AMP-PNP also resulted in a significant decrease in the co-localization of VBL-BPY and anti-Pgp mAb, indicating that the protein switched into a low substrate affinity conformation. Since AMP-PNP is a non-hydrolyzable ATP analogue, it can be assumed that ATP hydrolysis is not required for the decrease of the substrate affinity and the subsequent release of the substrate.

In the case of single Walker A mutant Pgp expressing cells the AMP-PNP caused smaller decrease in VBL-BPY binding compared to wild type Pgp expressing cells. In contrast, simultaneous mutation of both Walker A lysine residues resulted in a permanent high drug binding affinity conformation, which could not be reversed by the addition of nucleotides.

4.7 Nucleotide binding reduces the UIC2 mAb reactivity of Pgp

As it was presented in the previous section, the non-hydrolysable ATP analogue AMP-PNP stabilized the Pgp molecules in low substrate affinity conformation. We wanted to know whether this conformation change can be detected by UIC2 mAb. Removal of nucleotides synchronized Pgp molecules in the UIC2-reactive conformation, while addition of AMP-PNP reduced the UIC2 staining. Based on it we can conclude that AMP-PNP binding to the NBDs induces a conformation change in TMDs simultaneously decreasing the UIC2 reactivity and substrate affinity of Pgp.

II. Investigation of inhibition mechanism of Pgp by UIC2 and its possible *in vivo* applications

4.8 Experimental strategy

To study the *in vitro* and *in vivo* effect of the combined application of UIC2, CsA and DOX, we used KB-3-1 human epidermoid carcinoma cell line and its vinblastine selected sub-clone, KB-V1. First, we wanted to know whether these cells are suitable for testing our Pgp inhibition strategy *in vivo*. Therefore, we determined the expression level of Pgp and other ABC transporters involved in the development of multidrug resistance (ABCG2 and ABCC1) in the KB cell line pair. The KB-3-1 and KB-V1 cells were injected subcutaneously into SCID mice, which were then treated with DOX, UIC2 and CsA or their combination on the fourth day of the experiment. Since palpable tumors were grown in the untreated mice by the twelfth day, we terminated the experiment, removed the tumors from the mice and determined their mass and compared their Pgp expression to that of the tumor cells used for grafting the tumors.

4.9 KB-V1 cells express Pgp at high level

Before we started *in vivo* experiments, we determined the cell surface expression level of the ABC transporters that are the most often responsible for the multidrug resistance (Pgp, ABCG2 and MRP1) in both cell lines. In the case of KB-3-1 no Pgp expression could be detected, while KB-V1 cells expressed Pgp at high level. Besides this neither ABCG2 nor ABCC1 (both has overlapping substrate spectrum with the Pgp) expression were detected in the cell lines.

4.10 Pgp⁺ tumors retained their high Pgp expression level after xenotransplantation

To design a model system that is suitable for testing our *in vivo* Pgp inhibition strategy, we had to verify that the transplanted cells retain their original Pgp expression level in the course of the experiment. Due to the high growth rate of KB cells, palpable

subcutaneous tumors developed in 10–12 days after their xenotransplantation. Therefore, the experiment was terminated on the twelfth day. The tumors were removed and their Pgp mRNA level was determined by RT-qPCR and compared to those cells which were used for grafting the tumors. Pgp mRNA level of the KB-V1 tumors did not change upon proliferation of the inoculated cells, and it was at least three orders of magnitude higher than the Pgp mRNA level of the KB-3-1 cells. In the KB-3-1 tumors a well detectable ~60-fold increment of Pgp mRNA levels occurred compared to the inoculated cells, but it was still negligible compared to the KB-V1 tumors. Thus, the KB-V1 tumor xenografts retained their MDR phenotype, while the KB-3-1 cells continued to express Pgp at very low levels in the developed tumors on the time scale of the *in vivo* experiments.

Taken together the above model system can be suitable for testing our Pgp inhibition strategy *in vivo*.

4.11 UIC2 mAb in combination with low dose of CsA could restore the doxorubicin sensitivity of the Pgp⁺ cells to the level of the Pgp⁻ cells

To test our Pgp inhibition strategy and the KB-3-1/KB-V1 cell lines, we performed *in vitro* cytotoxicity tests. In accordance with the high Pgp expression level of KB-V1 cells were resistant to doxorubicin (DOX). The EC₅₀ value of DOX was 2.19±0.39 μM in these cells, while it was only 44±3 nM in KB-3-1 (Pgp⁻) cells. In KB-V1 cells CsA co-treatment decreased the EC₅₀ value of DOX in a dose dependent manner, while UIC2 had only a weak, statistically not significant effect. Interestingly, the combined treatment of KB-V1 cells with 1 μM CsA and a saturating concentration of UIC2 mAb decreased the EC₅₀ value to 33±19.7 nM, which was the sensitivity level of KB-3-1 cells. Similar decrease could be achieved by 10 fold higher CsA concentration when it was applied alone.

4.12 UIC2 mAb and CsA did not decrease the viability of KB cells neither used alone nor in combination

We tested whether UIC2, CsA or their combination has any effect on the cells viability *in vitro* in the absence of DOX. Administration of the UIC2 mAb and 1 μM CsA to cultures of KB-3-1 cells, simultaneously or alone, had no significant effects on their DOX sensitivity. Therefore, in accordance with previous data of our workgroup, we can conclude that the treatment with the combination of CsA and UIC2 takes effect by reducing the KB-V1 cells DOX sensitivity.

4.13 Combined treatment with DOX-CsA-UIC2 significantly decreased the growth rate of Pgp⁺ tumors

Based on the results discussed above, we designed *in vivo* experiments in which we investigated whether DOX in combination with low dose of CsA and UIC2 mAb is able to reduce the growth rate of the tumors in SCID mice that were developed from Pgp⁺ KB-V1 cells, which were injected subcutaneously into the animals. The animals were subjected to chemotherapy four days after the xenotransplantation, then eight days after chemotherapy, the animals were sacrificed by cervical dislocation and the tumors were

removed to weigh them. DOX treatment alone was almost ineffective in the case of KB-V1 tumors, while the weight of the KB-3-1 tumors decreased considerably. Co-administration of 10 mg/kg CsA decreased the size of the KB-V1 tumors only mildly and did not affect the KB-3-1 tumors. Combined treatment with DOX-CsA-UIC2 decreased the mean weight of the KB-V1 tumors 9 fold compared to the animals treated with DOX alone. The combined treatment also decreased the mean weight of the KB-3-1 tumors, but not in a statistically significant extent. Importantly, only 52% of the grafted Pgp⁺ or Pgp⁻ tumors developed into detectable tumors in the DOX-CSA-UIC2 treated animals, and 20% of the animals remained completely tumor-free. In contrast, we always detected tumors in the other treatment groups. Interestingly co-administration of UIC2 and DOX also decreased tumor size significantly compared to DOX alone in the case of KB-V1 tumors. This finding, in view of the fact that UIC2 treatment alone does not affect the EC₅₀ value of DOX in *in vitro* cytotoxicity tests, suggested to us that the growth inhibitory effect of the antibody is not exclusively due to Pgp inhibition, therefore, the contribution of the immune system, that is partly functional in the SCID mice, was tested.

4.14 UIC2 is able to trigger ADCC *in vitro*

We tested whether UIC2 is able to induce antibody-dependent cell-mediated cytotoxicity (ADCC) or complement-dependent cytotoxicity (CDC). Since the experiments required a huge number of living immune cells, which could be obtained by sacrificing too many mice, we used human immune cells and serum instead.

PBMCs killed about 70-80% of the UIC2 treated KB-V1 cells both in the presence and absence of CsA, at target to effector cell ratios of 1:50 and 1:100, respectively, in contrast with the UIC2 treated KB-3-1 cells that exhibited a survival rate similar to that of the untreated control. In the absence of UIC2, the percentages of dead target cells were low. In *in vitro* CDC experiments cell killing did not increase in the UIC2 treated KB-V1 and KB-3-1 samples despite the applied sera showed strong hemolytic activity in the control experiments. Based on these result we could assume that binding UIC2 to the Pgp⁺ cells induced ADCC but no CDC.

5 Discussion

I. Examination of substrate binding ability of P-glycoprotein during the catalytic cycle

Based on crystal structures and a wealth of biochemical and biophysical data it is generally accepted that ABC transporters have at least two discrete, energetically stable conformations: one with dissociated NBDs that is opened toward the cytoplasm and another with dimerized NBDs and rearranged TMDs opened toward the extracellular space. The switch between the two states presumably involves a series of conformational changes which ultimately result in the reduction of substrate binding affinity required for uphill substrate transport. The exact molecular mechanisms that link nucleotide binding to the association and dissociation of NBDs and to the conformational changes of the TMDs that result in changes in substrate affinity are not fully understood. In the present study we correlated UIC2-reactivity with drug binding affinity for wild-type and mutant Pgp variants in permeabilized cells to elucidate the link between ATP binding, hydrolysis and the conformational rearrangements responsible for switching the affinity of the substrate binding sites during substrate transport.

We used the UIC2 conformation sensitive mAb to detect molecular movements in the TMDs of the Pgp and we obtained information about the substrate affinity of the Pgp by measuring the co-localization between the fluorescence signals of VBL-BPY and 15D3-A647 at different stages of the catalytic cycle. In view of the intimate association of Pgp with the lipid bilayer in which it is embedded, and from which it harvests its substrates, the strength of our experimental systems that they provide information about the transporter in its natural plasma membrane environment.

Our results demonstrated that AMP-PNP binding is sufficient to induce the conformational switch corresponding to the transition from the inward to the outward facing conformation that can be detected by UIC2 mAb. Using the same experimental setup, we also showed that binding of AMP-PNP switches Pgp into the low drug binding affinity state. The simultaneous drop in the UIC2- and drug-binding affinities suggests that the transition from the inward- to the outward-facing conformation precedes ATP hydrolysis in any case.

Residues of the Walker motifs in each NBD, together with the signature sequence of the contralateral NBD, directly participate in nucleotide-dependent dimerization of the two NBDs and ATP hydrolysis. But how ATP hydrolysis is coordinated between the two NBDs, and whether Pgp hydrolyses one or two (or more) ATP molecules per each transported substrate are not known. Based on literature, mutations of the conserved Walker A lysine reduce ATPase activity to very low levels in diverse ABC transporters. The two nucleotide binding domains of Pgp were shown to be functionally equivalent and the integrity of both catalytic centers is generally believed to be needed for transport, because inactivation of a single NBD results in inhibition of ATPase and transport activities.

We confirmed that mutation of both Walker A lysine residues inactivates Pgp: as indicated by the lack of ATP-triggered conformational changes, the transporter is essentially frozen in the UIC2-reactive inward-open state characterized with high drug binding affinity. Intriguingly, however, our data showed that the inward-to-outward conformational switch can be triggered in the case of the single Walker A mutants together with the concomitant drop in drug binding affinity. Furthermore, we demonstrated that the stable Pgp-ADP-vanadate complex forms similarly in the WT and the unilateral Walker A mutant Pgp variants, which is characterized by low substrate affinity and low UIC2-reactivity. Other observations of our workgroup also support the idea, that the single Walker A mutants have catalytic activity: they have a low, but measurable ATPase activity that can be stimulated by substrates and their expression confers mild drug resistance to the cells. Based on our drug transport experiments we can tell that the single Walker A mutants have a 10-15 percent “residual” transport activity compared to the wild type, which can only happen if they are able to pass through the catalytic cycle repeatedly.

While our experimental system has several limitations, we note that the majority of the studies reporting the inactivating effect of single Walker A mutations have been performed using heterologous expression systems such as Sf9, *Saccharomyces cerevisiae* or purified and reconstituted proteins. It is known that the plasma membrane composition influences the catalytic activity of ABC transporters, and the amount of membrane cholesterol influences Pgp activity. Since membrane cholesterol levels are significantly lower in lower eukaryotes, it may be that the low ATPase activity of the single Walker mutants was missed due to the different plasma membrane composition of the heterologous expression systems, or artefacts related to the solubilization, purification and reconstitution of the proteins.

Our results are incompatible with catalytic cycle models supposing the hydrolysis of two ATPs per cycle. Similarly, our results are also difficult to reconcile with models suggesting that the two NBDs hydrolyze ATP in a strictly alternating order. If the NBDs were indeed recruited in a strictly alternating fashion, every second ATP would have to be processed by the mutant catalytic center, causing the cycle to stall. Instead, our results indicate that the wild-type catalytic site can hydrolyze ATP in repeated cycles without hydrolysis at the other NBD. The simplest interpretation of our data is that in WT Pgp one of the two functionally equivalent sites becomes committed to hydrolysis in each cycle on a random basis, whereas in the single mutants commitment of the only functional site initiates every cycle.

II. Investigation of inhibition mechanism of Pgp by UIC2 and its possible *in vivo* applications

Based on previous studies the UIC2 mAb can be used to inhibit Pgp mediated transport *in vitro* and *in vivo*. Similarly to other antibodies that exhibit conformation sensitive binding, UIC2 binds only to a small fraction of Pgps expressed in cell membrane. In the presence of certain modulators (e.g. CsA) applied at sub-inhibitory

concentrations all Pgp molecules become UIC2 reactive and therefore can be inhibited by the antibody. In our study we investigated whether the administration of UIC2 in combination with low-dose of modulator increases the effectivity of the chemotherapy.

To investigate the effect of the combined therapy *in vivo*, we designed a model system based on the xenotransplantation of the KB-3-1/KB-V1 Pgp⁻/Pgp⁺ human epidermoid carcinoma cells lines into SCID mice. In the above model system, co-treatment with UIC2 + CsA potentiated the anti-tumor effect of DOX and inhibited or hindered the development of KB-V1 Pgp⁺ tumors *in vivo*. At the same time, DOX treatment alone did not have a significant effect on the size of the KB-V1 tumors. These data are in line with the conclusions of our previously published *in vitro* and *in vivo* drug accumulation studies and with the results of the *in vitro* cytotoxicity measurements. However, in contrast with the *in vitro* cytotoxicity tests, in our *in vivo* experiments treatment with UIC2 alone also decreased the growth rate of the Pgp⁺ tumors. These observations may suggest that the dramatic antitumor effect of the combined treatment is not the exclusive result of increased antibody binding with consequential Pgp inhibition and DOX accumulation, the mechanism is more complex. Therefore, the differences between the results of the *in vitro* cytotoxicity tests and *in vivo* experiments carried out on SCID mice raised the possibility that immunological processes could contribute to the cytotoxic effects of our treatment protocol.

SCID mice, regardless their adaptive immune system is dysfunctional, have intact complement system as well as functioning macrophages, natural killer cells and polymorphonuclear cells. Therefore, antibody binding to the tumor cells may elicit cytotoxicity directly through complement binding (complement-dependent cytotoxicity, CDC) or indirectly, via the recruitment of the above effector cells to the antibody covered tumor cells (antibody-dependent cell-mediated cytotoxicity, ADCC). Our *in vitro* ADCC assays supported the notion that the UIC2 mAb induces ADCC *in vivo* in the SCID mice.

The involvement of ADCC in the *in vivo* anti-tumor effect of UIC2 treatment is an unexpected finding of our experiments. IgG₂ antibodies, which UIC2 belongs to, are mostly inefficient at supporting effector functions and are chosen for antibody therapy when effector functions are unnecessary or undesirable. Since IgG₂ isotype antibodies do not trigger natural killer cell mediated ADCC, therefore in our *in vitro* ADCC experiments carried out with PBMCs cell killing was mediated by monocytes. Since SCID mice also have monocytes the same mechanism is functional and probably explains our *in vivo* results.

The above results raise the question whether the strong anti-tumor effect of the combined treatment might be attributed exclusively to ADCC triggered by the UIC2 mAb binding. However, the fact that the extents of the *in vitro* ADCC effects were indistinguishable in the presence of UIC2 or UIC2+CsA suggests that binding of the antibody to a small fraction of the cell surface Pgps (20-40%) is sufficient to induce a maximal ADCC effect. Consequently, the differences in the size of the KB-V1 tumors

between the UIC2 and UIC2+CsA treated animals and the lack of the KB-V1 tumors in 52% of these animals argue against the above assumption and suggests that the stronger Pgp inhibitory effect of the UIC2+CsA combination mediates the anti-tumor effect at least in part. This hypothesis is supported by previous studies of our workgroup in which a two fold increase in the accumulation of a Pgp substrate daunorubicin (also a Pgp substrate cytostatic drug) was measured 8 hours after the injection of UIC2 and CsA added at similar conditions. Taken together, our *in vitro* and *in vivo* data suggest that strong anti-tumor effect can be reached by the combinative treatment studied, as a joint result of Pgp inhibition and ADCC.

ADCC can be triggered at relatively low receptor occupancy by the antibody or at low receptor abundance. Thus, the 60 fold increased Pgp expression level of the KB-3-1 tumors compared to the KB-3-1 cells is probably sufficient to trigger ADCC effect, when the Pgp molecules are saturated by the antibody in the presence of CsA. In line with this assumption in 52% of the DOX-UIC2-CsA treated animals we could not detect KB-3-1 tumors, while they appeared in all of the DOX or DOX+UIC2 treated animals.

The Pgp specific nature of the observed effects was proved by our observation that decreased tumor size was detected exclusively in those animal groups that received UIC2 mAb treatment. In addition, in our previous studies we compared the KB-V1 cell line with *mdr1* transfected NIH 3T3 murine fibroblast cells, and Pgp⁺ A2780AD ovarian carcinoma cells and found them equivalent in every aspect of their multidrug resistant phenotype including the inhibition of Pgp-mediated drug transport by UIC2 mAb. On the other hand, ADCC effect is not dependent on the tissue origin of the target cells; rather it is determined by the interaction between the Fc part of the antibody and the Fc receptor of the effector cells.

Doubts about the possible clinical application of an anti-Pgp mAb based tumor therapy are related to the likely side effects that may arise as a result of either Pgp inhibition or ADCC, both exerted on cells expressing Pgp at physiological barriers of the body. For instance, inhibition of Pgp expressed in the blood-brain barrier may lead to increased accumulation of its substrates in the central nervous system leading to neurotoxicity (as it was experienced in *mdr1a/b* knock-out mice). However, administration of Pgp modulators in clinical trials does not seem to cause toxicity to the central nervous system probably because other ABC transporters (e.g. MRP1, BCRP1) may compensate for the loss of Pgp's function. However, in contrast to Pgp inhibition, ADCC is more dangerous, because it may damage the tissues at the physiological Pgp expression sites. Since ADCC is mediated via the Fc portion of the antibody, to avoid this side-effect upon human applications the whole UIC2 antibody could be substituted for by its Fab fragments. Upon humanization of the antibody its effector functions may be also fine-tuned by the design of the Fc part.

The UIC2 mAb does not bind to mouse Pgp, therefore the SCID mouse model system is not applicable for studying the possible side effects brought about by antibody binding to physiological Pgp expression sites. Since the UIC2 mAb also recognizes

primate and sheep Pgp, such animal models may be used for the evaluation of the feasibility of the strategy demonstrated herein. Direct injection of the antibody into the tumor tissue may also be tested for the purposes of reducing antibody dose and decrease systemic side effects.

In our model system, treatments were applied shortly, four days after injection of the tumor cells, when the tumors were still rather small, the situation perhaps analogous to the clinical setting when systemic therapy is applied to prevent or hinder the development of multidrug resistant metastatic tumors.

Each multidrug resistant tumor may have a unique signature of resistance mechanisms. Consequently, cancer therapy will need to be personalized, not only with respect to the mechanisms of malignant transformation or the tissue origin of the tumor but also regarding to the mechanisms of resistance. The strategy of Pgp inhibition demonstrated herein is offered to enrich the repertoire of possible protocols that can be considered for the treatment of multidrug resistant tumors, once humanized UIC2 becomes available.

5.1 Summary

- ❖ We have developed a fluorescence co-localization measurement based assay to detect the changes of the substrate affinity of Pgp upon distinct phases of its catalytic cycle. In addition, we adopted numerous fluorescence based techniques to measure the transport activity and conformation changes of Pgp. Using the mentioned assays we made the following statements regarding the catalytic mechanism of Pgp:
 - The conformation change of Pgp from the inward open, high substrate affinity state to the outward open, low substrate affinity conformation precedes the ATP hydrolysis.
 - The double Walker A mutant Pgp variant is catalytically inactive and trapped in the inward open, high substrate affinity conformation.
 - Single Walker A mutants have significant residual transport activity and thus they are capable of passing through full transport cycles, albeit with reduced efficiency.

- ❖ We designed an *in vivo* model system based on the xenotransplantation of Pgp-positive and Pgp-negative human tumors into SCID mice to test whether the combined treatment with low dose of CsA and UIC2 mAb can potentiate the anti-tumor effect of doxorubicin.
 - Our results demonstrated that the combined treatment significantly increased the sensitivity of the Pgp expressing tumors to doxorubicin and decreased the growth rate of the tumors at a clinically relevant extent.
 - We also concluded that antibody-dependent cell-mediated cytotoxicity (ADCC) contributes to the anti-tumor effect of the combined treatment *in vivo*, besides Pgp inhibition.



Registry number: DEENK/76/2018.PL
Subject: PhD Publikációs Lista

Candidate: Gábor Szalóki

Neptun ID: EPEUDY

Doctoral School: Doctoral School of Molecular Cellular and Immune Biology

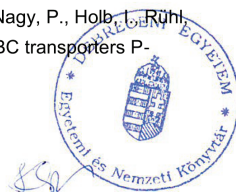
MTMT ID: 10040820

List of publications related to the dissertation

1. Bársony, O.*, **Szalóki, G.***, Türk, D., Tarapcsák, S., Gutay-Tóth, Z., Bacsó, Z., Holb, I., Székvölgyi, L., Szabó, G., Csanády, L., Szakács, G., Goda, K.: A single active catalytic site is sufficient to promote transport in P-glycoprotein.
Sci. Rep. 6 (24810), 1-16, 2016.
DOI: <http://dx.doi.org/10.1038/srep24810>
* These authors contributed equally to this work.
IF: 4.259
2. **Szalóki, G.**, Krasznai, Z. T., Tóth, Á., Vízkeleti, L., Szöllősi, A. G., Trencsényi, G., Lajtos, I., Juhász, I., Krasznai, Z., Márián, T., Balázs, M., Szabó, G., Goda, K.: The strong in vivo anti-tumor effect of the UIC2 monoclonal antibody is the combined result of Pgp inhibition and antibody dependent cell-mediated cytotoxicity.
PloS ONE. 9 (9), 1-9, 2014.
DOI: <http://dx.doi.org/10.1371/journal.pone.0107875>
IF: 3.234

List of other publications

3. Tarapcsák, S., **Szalóki, G.**, Telbisz, Á., Gyöngy, Z., Matúz, K., Csősz, É., Nagy, P., Holb, I., Rühl, R., Nagy, L., Szabó, G., Goda, K.: Interactions of retinoids with the ABC transporters P-glycoprotein and Breast Cancer Resistance Protein.
Sci Rep. 7 (41376), 1-31, 2017.
DOI: <http://dx.doi.org/10.1038/srep41376>
IF: 4.259 (2016)





4. Hoffmann, O. I., Kerekes, A., Lipták, N., Hiripi, L., Bodó, S., **Szalóki, G.**, Klein, S., Ivics, Z., Kues, W. A., Bősze, Z.: Transposon-Based Reporter Marking Provides Functional Evidence for Intercellular Bridges in the Male Germline of Rabbits.
PLoS One. 11 (5), 1-15, 2016.
DOI: <http://dx.doi.org/10.1371/journal.pone.0154489>
IF: 2.806
5. Trencsényi, G., Kertész, I., Krasznai, Z. T., Máté, G., **Szalóki, G.**, Péli-Szabó, J., Kárpáti, L., Krasznai, Z., Márián, T., Goda, K.: 2' [18F]-fluoroethylrhodamine B is a promising radiotracer to measure P-glycoprotein function.
Eur. J. Pharm. Sci. 74, 27-35, 2015.
DOI: <http://dx.doi.org/10.1016/j.ejps.2015.03.026>
IF: 3.773
6. Krasznai, Z. T., Trencsényi, G., Krasznai, Z., Mikecz, P., Nizsalóczi, E., **Szalóki, G.**, Péli-Szabó, J., Balkay, L., Márián, T., Goda, K.: 18FDG a PET tumor diagnostic tracer is not a substrate of the ABC transporter P-glycoprotein.
Eur. J. Pharm. Sci. 64C, 1-8, 2014.
DOI: <http://dx.doi.org/10.1016/j.ejps.2014.08.002>
IF: 3.35
7. Trencsényi, G., Márián, T., Lajtos, I., Krasznai, Z., Balkay, L., Emri, M., Mikecz, P., Goda, K., **Szalóki, G.**, Juhász, I., Németh, E., Miklovicz, T., Szabó, G., Krasznai, Z. T.: 18FDG, [18F]FLT, [18F]FAZA and 11C-methionine are suitable tracers for the diagnosis and in vivo follow up the efficacy of chemotherapy by miniPET both in multidrug resistant and sensitive human gynecologic tumor xenografts.
Biomed Res. Int. 2014, 1-10, 2014.
DOI: <http://dx.doi.org/10.1155/2014/787365>
IF: 1.579
8. **Szalóki, G.**, Czégény, I., Szemán-Nagy, G., Bánfalvi, G.: Removal of Heavy Metal Sulfides and Toxic Contaminants from Water.
In: Cellular effects of heavy metals. Ed.: Gáspár Bánfalvi, Springer, Milton Keynes, 333-346, 2011.

Total IF of journals (all publications): 23,26

Total IF of journals (publications related to the dissertation): 7,493

The Candidate's publication data submitted to the iDEa Tudóster have been validated by DEENK on the basis of Web of Science, Scopus and Journal Citation Report (Impact Factor) databases.

22 March, 2018

